scientific reports

Check for updates

OPEN

ASCL2 contributes to clinical assessments of breast cancer and mediates tumor progression via the interaction with CLDN3

Yulong Yin[1], Qingjie Meng[1], Xianghua Liu[1], Fangshi Xu[2], Yiwen Li[3], Xiaogang Han[1], Qianqian Guo[4] & Yonggang Lv[1]✉

Breast carcinoma (BC) is the most common malignant neoplasm occurring in women, posing a serious threat to public health. Metastasis is its leading cause of death, nevertheless there is still a lack of effective treatment. Epithelial-mesenchymal transition (EMT) is a critical process involved in cancer malignant progression, which is expected to provide new insights into BC treatment. Through lasso regression SVM-RFE algorithms, ASCL2 was identified as a potential regulator for BC progression. Multi-omics bioinformatics investigation confirmed its great value in clinical assessments. ASLC2 can elevate the decision-making benefit of TNM and AJCC-stage prognostic models and distinguish the prognostic differences of patients with different molecular subtypes. A survival meta-analysis confirmed its prognostic value in five public cohorts. High expression of ASCL2 was associated with unfavorable anti-tumor immune response as determined by CIBERSORT algorithm and immunofluorescence staining. Meanwhile, ASCL2 was also indicative of metabolic status and therapeutic efficacy through GSEA, GDSC, TIDE and TMB analyses. As for its biofunctions, overexpression of ASCL2 promoted proliferation, migration and invasion of MCF-7 and MDA-MB-231 cells. Silencing ASCL2 can significantly inhibit the growth of xenograft tumors in mice. Mechanistically, CLDN3 was predicted to have a close functional link with ASCL2 through module and spearman analyses. Co-IP assay confirmed the interaction of ASCL2 and CLDN3. Rescue experiments demonstrated that overexpression of CLDN3 could partly reverse the inhibitory effects of ASCL2 deletion on the malignant capacities of BC cells, suggesting their synergistic effects. Collectively, ASCL2 is a pivotal biomarker for successful individualized cancer therapy, targeting ASCL2 has enormous therapeutic potential.

Keywords Breast cancer, Epithelial-mesenchymal transition, ASCL2, CLDN3, Prognosis

Despite recent advances in therapeutic and diagnostic approaches, breast invasive cancer (BRCA) remains the most common malignant tumor in women and the second leading cause of cancer-related death in women[1]. The incidence of BRCA continues to trend upwards, increasing by 1% each year from 2012 to 2021[1]. Therefore, it poses a serious health threat and economic burden to the public[2]. Although surgery combined with endocrine and molecular targeted therapies greatly improves the prognosis of patients, leading to a 5-year overall survival rate (OSR) of up to 87% for patients with clinical stage I and II, there are still many dilemmas in the current treatment and clinical assessments of BRCA. For instance, BRCA is highly heterogeneous, and triple-negative breast cancer (TNBC) is its refractory subtype. For the metastatic TNBC, the median progression-free survival (PFS) of patients receiving pembrolizumab plus chemotherapy is only 7.6 months[3]. Hence, in-depth investigation of the molecular mechanisms involved BC malignant progression is of great significance.

Epithelial-mesenchymal transition (EMT) is a biological process characterized by the acquisition of mesenchymal properties by epithelial cells[4]. There is ample evidence that EMT profoundly affects tumor

[1]Department of Thyroid and Breast Surgery, The Affiliated Hospital of Northwest University, Xi'an No.3 Hospital, No.10, Fengcheng Third Road, Weiyang District, Xi'an 710018, Shaanxi, China. [2]Department of Vascular Surgery, The Second Affiliated Hospital of Xi'an Jiaotong University, No.157, West Five Road, Xi'an 710004, Shaanxi, China. [3]Department of Biology, Georgetown University, Regents Hall, Room 406, 37Th and O St, NW, Washington DC 20057, USA. [4]Department of Imaging, The Affiliated Hospital of Northwest University, Xi'an No.3 Hospital, No.10, Fengcheng Third Road, Weiyang District, Xi'an 710018, Shaanxi, China. ✉email: lvygmedicine@163.com

metastasis, invasion and therapeutic resistance[5]. For instance, PD-L1 knockdown can suppress the angiogenesis of non-small cell lung cancer (NSLC) through retarding ZEB1-triggered EMT[6]. CD147 promotes BRCA progression through inducing EMT via the MAPK/ERK signaling pathway[7]. Clearly, with in-depth research, targeting EMT stepwise becomes a promising direction to curing human cancers[8]. Among the numerous EMT regulators, ASCL2 has attracted extra attention from oncology researchers due to its critical roles in multiple biological processes in human cancers. For example, ASCL2 can not only induce an immune excluded microenvironment, but also affect the efficacy of immunotherapy in colorectal cancer (CRC)[9,10]. Regrettably, its action mechanisms in BRCA tumorigenesis remain poorly characterized.

Despite no direct evidence confirming the linkage between ASCL2 and EMT, the own functional attributes of ASCL2 reveal the potential connection between the them. On one hand, ASCL2 can enhance the activity of the Wnt/β-catenin pathway, which is one of the core signaling pathways regulating the EMT process[11]. Mechanistically, ASCL2 can bind to the promoter region of the TCF7L2 gene, which is the most important member of the TCF/LEF family and is essential for β-catenin into the nucleus[12]. On the other hand, ASCL2 is affiliated with the basic helix-loop-helix (bHLH) family of transcription factors (TFs), which can activate transcription by binding to the E box and plays critical roles in regulating cellular proliferation, differentiation and phenotype maintenance[13]. For example, E47, a classical member of bHLH family, has been confirmed to be indispensable in the maintenance of EMT through directly binding to the promoter of E-cadherin[14]. TWIST1, another well-known member of bHLH family, serves as a pivotal TF responsible for promoting EMT[15]. Therefore, ASCL2 may be also strongly implicated in EMT regulation. Indeed, the evidence from gastric cancer (GC) and colorectal cancer (CRC) have both confirmed its facilitative roles in EMT process[16,17].

Herein, we utilized two machine learning algorithms to identify ASCL2 as a potential biomarker for driving BRCA progression and characterizing its clinical status. With the aid of comprehensive data mining, the pivotal values of ASCL2 in clinical assessments of BRCA were also determined, such as the prediction of survival outcomes and therapeutic responses. Moreover, ASCL2 exhibited potent carcinogenic abilities both in vivo and in vitro, showing great potential as a novel therapeutic target. Mechanistically, the interaction of ASCL2 and CLDN3 drove BRCA tumorigenesis. Our findings provide new insights into BRCA treatment and contribute to its individualized therapy.

Materials and methods

Data source

The transcriptome data and clinical information of five public cohorts were utilized for data mining, including TCGA-BRCA, MEABRIC, ICGC-KR, GSE20685 and GSE42568 datasets. Their brief information and main use were presented in Table 1. Their clinical characteristics were shown in Table S1. All transcriptome data was standardized by log2 (FPKM + 1) transformation.

EMT-related gene set

EMTome (www.emtome.org) and MSigDB databases (https://www.gsea-msigdb.org/) provided an EMT-related gene set consisting of 1072 regulatory genes[18]. Among that, three EMT-related gene sets contributed to this establishment process, including 'HALLMARK Epithelial to mesenchymal transition', 'GOBP Epithelial to mesenchymal transition', and 'GOBP Regulation of epithelial to mesenchymal transition' (Table S2). The protein–protein interaction (PPI) network of these EMT genes was constructed using the STRING database and their biological functions were analyzed using Metascape database[19,20].

Consensus clustering and machine learning analysis

Consensus clustering analysis was performed via the 'ConsensusClusterPlus' package in R software (version 4.3.3). The optimal number of clusters was determined according to the cumulative distribution function (CDF). The heatmap of the consistency matrix was employed to quantify the intragroup and intergroup heterogeneities. Lasso regression and support vector machine recursive feature elimination (SVM-RFE) was used to identify the pivotal EMT genes involved in BRCA pathogenesis. The former machine learning algorithm was performed via 'glmnet' R package, and the latter one was 'KeBABS' R package.

Prognostic analysis

According to the cutoff value of ASCL2 expression, BRCA patients in each public cohort were divided into high- and low-ASCL2 expression groups. The cutoff value was determined using the Cutoff Finder online tool. The survival difference analyses were based on the Kaplan–Meier method. A series of prognostic analyses were conducted to assess the clinical value of ASCL2, including receiver operating characteristic curve (ROC), multivariate independent prognostic analysis, decision curve analysis, clinical subgroup analysis, and

Cohort	Sample size	PMID	Platform	Main use
TCGA-BRCA	1015	NA	NA	Prognostic, immune, metabolic and therapeutic status
METABRIC	1764	22,522,925	Illumina HT-12 v3	Prognostic validation
ICGC-KR	50	NA	Illumina HiSeq 2000	Prognostic validation
GSE20685	327	25,887,482	GPL570	Prognostic validation
GSE42568	104	23,740,839	GPL570	Prognostic validation

Table 1. Brief information and main uses of five public cohorts. NA, not applicable.

nomogram. A meta-analysis was conducted using Review Manager 5.2 software to assess the comprehensive prognostic effect of ASCL2 across multiple cohorts. The evaluation indicator was odds ratio (OR) value. I^2 value was applied to measure statistical heterogeneity. The overall effects were tested by z test.

Immune analysis and immunofluorescence assay

The immune effects of ASCL2 were explored using CIBERSORT algorithm, ESTIMATE method, ssGSEA and TIMER online tool[21–23]. Next, we conducted immunofluorescence to validate the effects of ASCL2 on the infiltration levels of CD8 + T cells. The experimental workflow followed as previously reported[24]. Briefly, the 4-mm tissue sections prepared were sequentially subjected to dewaxing, antigen retrieval, fixation, and nonspecific blocking. Then, tissue sections were incubated with first and secondary antibodies (ASCL2: ab157918, CD8: ab33786, Abcam, Cambridge, UK) in a light avoidance condition. ASCL2 was stained by the FITC-labeled goat anti-mice IgG (H&L) antibody (Beyotime, Shanghai, China). CD8 was stained by the Cy3-labeled goat anti-mice IgG (H&L) antibody. Nucleus was stained by the Hoechst reagent (Beyotime, Shanghai, China). The stained slides were observed via a fluorescent microscope under a 40 × magnification (Olympus BX53).

GSEA

Metabolic analysis was performed using gene set enrichment analysis (GSEA). Nine gene sets used in GSEA were obtained from MSigDB database and listed in Table S3. The phenotype labels were high-ASCL2-expression samples versus low-ASCL2-expression samples. A total of 1000 permutations were performed with no gene symbol collapse.

Therapeutic correlation analysis

Genomics of Drug Sensitivity in Cancer (GDSC) database was used to investigate the relationships between the ASCL2 expressive levels and the sensitivity of molecular targeted therapy (MTT) and multiple chemotherapy drugs. The predictive role of ASCL2 on the efficacy of immune checkpoint inhibitors (ICIs) was assessed using tumor mutation burden (TMB)[25], TIDE score[26], expressions of immune checkpoints (ICs), and IMvigor 210 cohort[27].

Clinical samples and RT-qPCR

25 pairs of BRCA and adjacent normal tissues were collected from the department of breast and thoracic surgery in Xi'an No.3 hospital (May 15th, 2023 to May 15th, 2024). All parents have signed the informed consent before PCR detection. The study protocol was approved by the Ethics Committees of Xi'an No.3 Hospital (ID:20,230,416). We confirmed that all methods were performed in accordance with the relevant guidelines and regulations.

Total RNA was extracted using TRIzol Reagent (TakaRa, Japan). The optical density at 260 nm and 280 nm (A260/A280) was measured for evaluating RNA purity of samples. Reverse transcription was conducted using PrimeScript RT reagent Kit (Takara, Japan). On the ABI Prism 7900 sequence system, PCR reaction was labeled and detected using SYBR-Green PCR Reagent (Takara, Japan). GAPDH was used as the internal reference. The relative gene expression was calculated according to the 2-ΔΔCT method.

Western blot

Western blot assays were conducted as previously reported[24]. Briefly, cells were lysed using RIPA buffer (Beyotime, China). The protein concentration was measured using BCA kit (Beyotime, China) and the proteins were separated by 10% SDS-PAGE (Applygen, China). The membranes were blocked by 5% of skim milk and incubated with primary and secondary antibodies. The used antibodies (Sigma-Aldrich, German) were as follows: anti-ASCL2 rabbit polyclonal antibody (1/1000, SAB1305026), anti-CLDN3 rabbit monoclonal antibody (1/1000, CL13128), anti-GAPDH rabbit polyclonal antibody (1/2500, ABS16). Protein blots were visualized by BeyoECL plus solution (Beyotime, China).

Cell culture and gene vectors

Two breast cancer cell lines (MCF-7 and MDA-MB-231) were purchased from Procell Life Company (Wuhan, China). MCF-7 cells were cultured in MEM medium containing 10% FBS (Fetal bovine serum) and 1% P/S (Penicillin/ Streptomycin). MDA-MB-231 cells were cultured in Leibovitz's L-15 medium containing 10% FBS and 1% P/S. Cells were incubated at 37℃ and 5% CO2. Specific short hairpin RNAs (sh-ASCL2 and sh-CLDN3) and overexpression plasmids (OE-ASCL2 and OE-CLDN3) were synthesized by HanHeng Biotechnology (Shanghai, China).

Colony formation assay

Cell proliferation was assessed by colony formation assay. In a 6-well plate, the cells with logarithmic growth phase were seeded at a density of 1.5×10^3 cells/ per well. When colonies formed, they were fixed and stained using methanol and Giemsa. Colonies were counted under the microscope from five random fields.

Transwell migration and invasion assays

The experimental flow was referred to previous studies[22]. To perform migration assays, the upper chambers were added medium with 0.1% FBS, while the lower chambers were added medium with 10% FBS. 5×10^3 cells were seeded into upper chamber for 24-h incubation. Then, unmigrated cells were removed by PBS and cotton swab. Migrated cells were fixed and stained by paraformaldehyde and 0.1% crystal violet. In invasive assays, the upper chambers were precoated with Matrigel (Corning, NY, USA). Quantitative analysis was conducted using a high magnification microscope (100-fold) from five random visual fields.

Co-Immunoprecipitation (Co-IP)

Protein A + G Agarose (Beyotime, China) was used to conduct this experiment, which followed the protocol of manufacturer. Briefly, protein A/G magnetic beads were bound and crosslinked by DSS to the first antibody. Cells were lysed and incubated with beads overnight. Afterward, bound antigens were eluted from the beads by sample buffer and detected using Western blot assay. The first antibodies were as follows: anti-ASCL2 rabbit polyclonal antibody (1/1000, SAB1305026), anti-CLDN3 rabbit monoclonal antibody (1/1000, CL13128).

Xenograft assay

Ten female BALB/c nude mice were purchased from Animal Experimentation Center, Xi'an Jiaotong University School of Medicine, and were applied for in vivo experiment. 1×10^7 MCF-7 cells transfected with sh-ASCL2 or sh-vector were subcutaneously injected into the right flank of each mouse. The length and width of xenograft were measured every four days, by which tumor volume was calculated according to the formula: $0.5 \times (\text{tumor length}) \times (\text{tumor width})^2$. Mice were anesthetized with ketamine. After the mice were sacrificed by cervical dislocation, tumors were harvested and weighed. This study was approved by the Ethics Committee of Xi'an No.3 Hospital (ID:20,230,416). We confirmed that all methods were carried out in accordance with relevant guidelines and regulations. We confirm that all methods are reported in accordance with ARRIVE guidelines.

Statistical analysis

All statistical analyses were performed using the R software (Ver 4.3.3) and GraphPad Prism (Ver 9.0). The continuous variables among groups were compared using the T test or Welch T test. The categorical variables among groups were compared using the Wilcoxon rank sum test. Spearman coefficient was applied in correlation analysis. In vitro experiments were conducted three times independently. $P < 0.05$ was considered statistically significant.

Results

ASCL2 is a potential gene for characterizing the EMT prognostic risk in breast carcinoma

The flowchart of this study was shown in Fig. 1. EMTome and MSigDB databases were employed to construct an EMT-related gene set containing 1072 members (Fig. 2A). The PPI network of these EMT genes was presented in Fig. 2B. Biological function analysis confirmed that they enriched in EMT process, including 'regulation of epithelial mesenchymal transition' and 'Extracellular matrix organization' (Fig. 2C). Consensus clustering analysis which defined the prognosis of BC patients (TCGA-BRCA cohort) as the outcome variable revealed that 1072 EMT genes could be divided into four patterns (Fig. 2D). Regrettably, four EMT clusters could only reflect 44.2% of the prognostic alteration (Fig. 2E), and there was no significant difference in OSR of patients

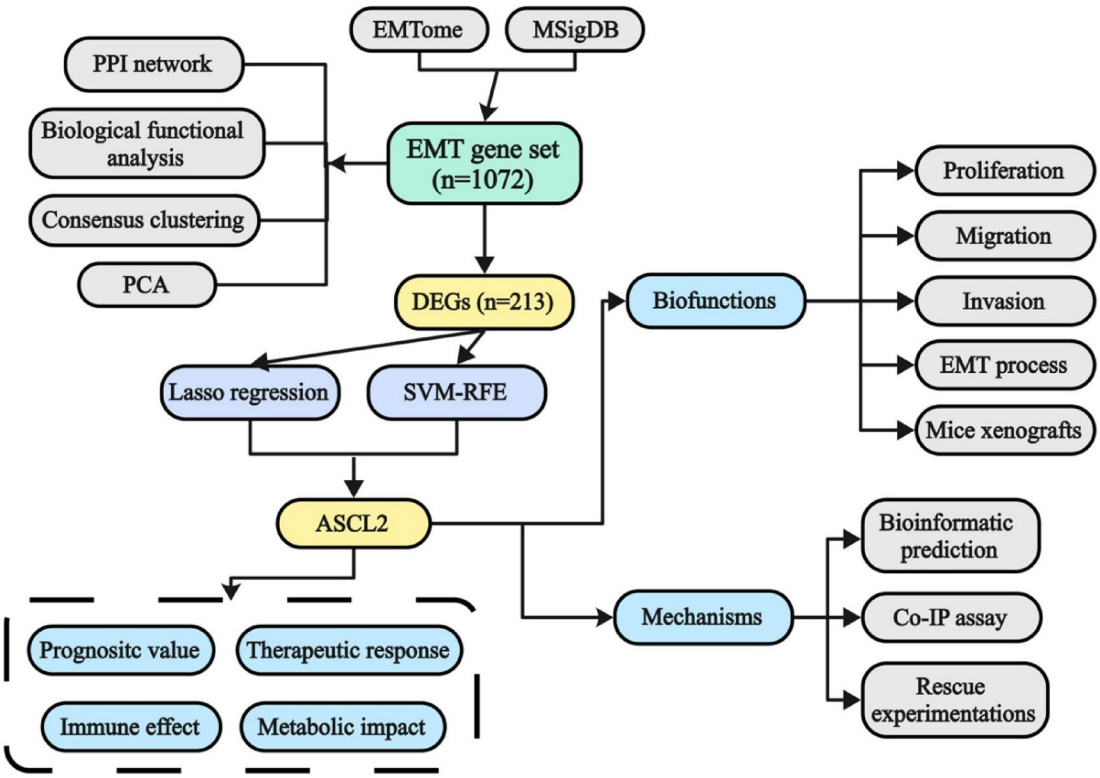

Fig. 1. The workflow of this study. EMT, epithelial-mesenchymal transition; PPI, protein–protein interaction; PCA, principal components analysis; DEGs, differentially expressed genes; SVM-RFE, support vector machine-recursive feature elimination; Co-IP, Co-Immunoprecipitation.

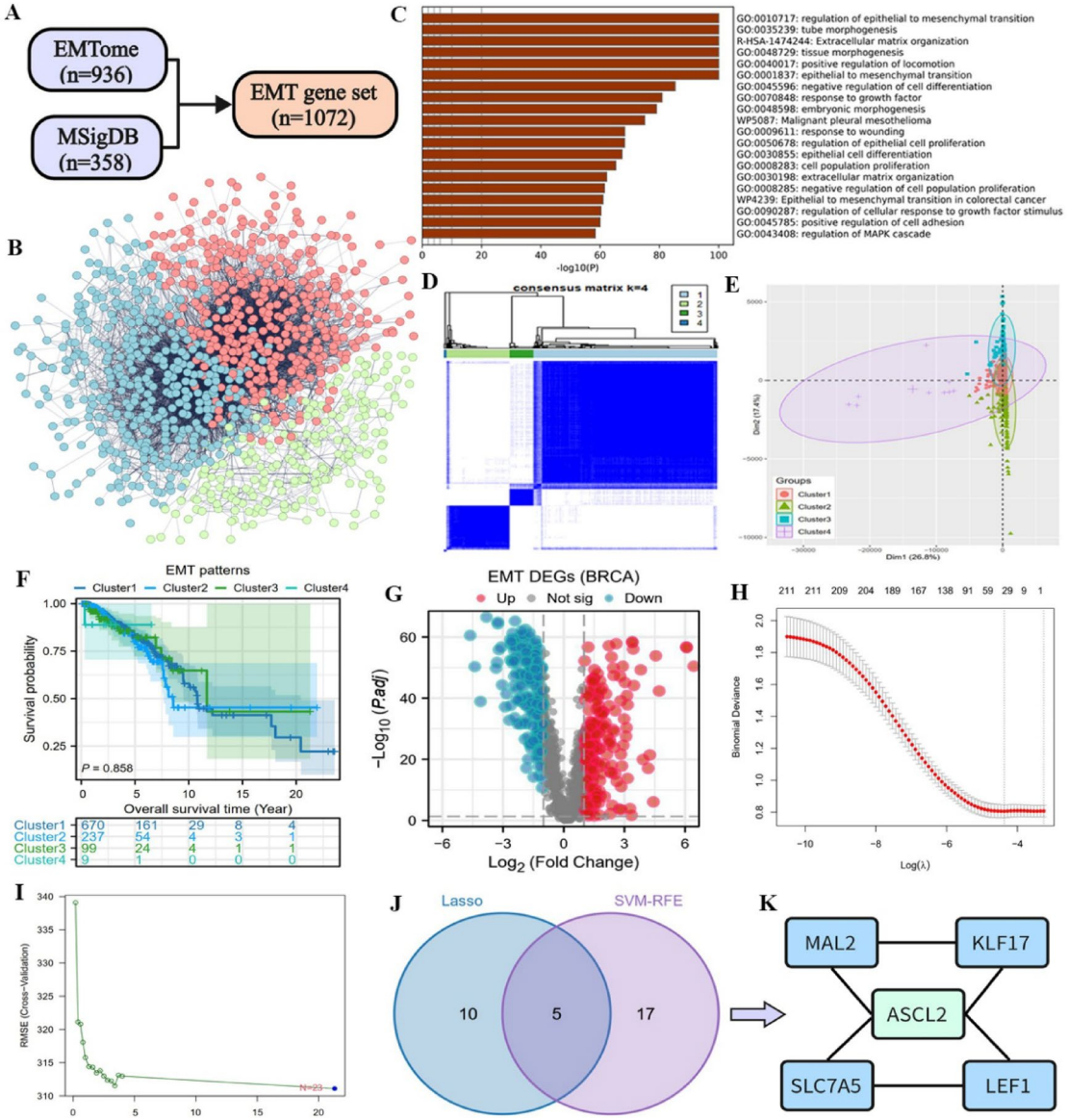

Fig. 2. Identification of critical EMT genes for characterizing breast carcinoma. (**A**) Construction of a comprehensive EMT gene set; (**B**) The PPI network of 1072 EMT regulators; (**C**) Function enrichment analysis of EMT gene set using Metascape database; (**D**) The results of consensus clustering analyses; (**E**) PCA results of four EMT clusters; (**F**) Survival differences between four EMT clusters (TCGA-BRCA cohort); (**G**) Differentially expressed genes between tumor and normal samples (the absolute value of Log2FC is greater than 1); (**H**) Lasso regression analysis; (I) SVM-RFE algorithm; (**J**) The intersection genes of two machine learning algorithms; (**K**) Five potential EMT genes affecting BC progression. BC, breast carcinoma.

with different clusters (Fig. 2F). Therefore, we attempted to apply machine learning algorithms to identify critical EMT genes that determine the prognosis of BRCA patients.

213 EMT genes with significant differential expressions in BC samples were identified using a volcano plot (Fig. 2G). Based on their expression matrix, 15 and 23 candidate genes were screened out respectively using lasso regression and SVM-RFE algorithms (Fig. 2HI). The intersection of two machine learning screening results yielded five candidate genes, including MAL2, KLF17, SLC7A5, LEF1 and ASCL2 (Fig. 2JK). Considering various research have witnessed the important roles of ASCL2 in multiple cancers (Table 2), ASCL2 was selected as the final research subject.

ASCL2 is of great value in prognostic assessment of BRCA patients

According to the cutoff value of ASCL2 expression (1.687), 1015 BRCA patients in TCGA cohort were divided into two groups. Patients with high ASCL2 expressions suffered from worse overall survival and progression free survival (PFS) time (Fig. 3AB). ASCL2 presented a good accuracy for predicting the OSR of BRCA patients (Fig. 3C) and was identified as an independent prognostic factor (HR = 1.227, Fig. 3DE). Notably, introducing

Cancer type	PMID	Expression	Function
Colon cancer	39,895,630	Up-regulated	Oncogenic properties
Colorectal cancer	37,591,954	Up-regulated	Immune excluded microenvironment
Colorectal cancer	36,824,410	Up-regulated	Stemness
Prostate cancer	38,064,349	Up-regulated	Neuroendocrine differentiation
Stomach adenocarcinoma	36,008,864	Up-regulated	Inflammation regulation
Pancreatic adenocarcinoma	38,955,307	Up-regulated	Oncogenic properties

Table 2. Critical functions of ASCL2 in human cancers.

ASCL2 as a prognostic variable can enhance the decision-making benefit of the TNM and AJCC-Stage models (Fig. 3F). The subgroup analyses showed that ASCL2 was able to distinguish prognostic differences among patients with different clinical features (Fig. 3G-M). For facilitating clinical practice, a nomogram consisting of age, clinical stage, molecular typing, and ASCL2 expressive level was constructed (Fig. 3N), and its prediction accuracy was approved by calibration curves (Figure S1).

Meanwhile, patients with high ASCL2 expressions were accompanied by the later TMN and clinical stages, indicating ASCL2 was involved in the malignant progression of BC (Fig. 4A). Moreover, Her-2 and luminal B types were more likely to appear in patients with high ASCL2 expressions, while the proportion of Basel and luminal A types were higher in low expression groups (Fig. 4B). There were obvious prognostic differences between high- and low-ASCL2 expression groups in patients with four molecular classifications (Fig. 4C-F). Collectively, ASCL2 provided valuable information for survival analyses of BRCA patients.

The prognostic value of ASCL2 is also successfully validated in other cohorts except for TCGA cohort

As expected, high ASCL2 expression also conferred an unfavorable survival outcome in METABRIC cohort (HR = 1.25, Fig. 4G). ASCL2 expressive levels were also associated with molecular classifications of breast carcinoma (BC) (Fig. 4H). The proportion of Her-2 and Claudin-low was significantly higher in high expression group, whereas that of luminal A and B types was markedly lower (Fig. 4H). However, ASCL2 can only distinguish the prognostic differences in luminal A and B types (Fig. 4IJ) but failed in other molecular classifications (Fig. 4K-M).

In GSE20685 and GSE42568 cohorts, ASCL2 still demonstrated prognosis discriminatory ability and moderate predictive accuracy ranging from 0.577 to 0.679 (Fig. 5A-D). Nevertheless, no prognostic differences were observed between different ASCL2 expression groups in ICGC-KR cohort, with an AUC value even less than 0.5 (Fig. 5EF). Ultimately, a meta-analysis combining five cohorts confirmed that high expression of ASCL2 increases the mortality risk of BC patients, with an odds ratio of 1.53 (Fig. 5G). No potential publication bias was detected through a funnel plot (Fig. 5H).

High expression of ASCL2 is a potential marker of adverse anti-tumor immune response

CIBERSORT algorithm revealed the complicated effects of ASCL2 on the levels of immune infiltration (Fig. 6A). Given that affected immune cells exert supportive or detrimental functions in anti-tumor response, high expressions of ASCL2 may ultimately result in immunosuppression (Table 3). Similarly, deep deletion of ASCL2 copy number strongly elevated the infiltration level of CD8 + T cells, which are the core cytotoxic cells in anti-tumor process (Fig. 6B). The immunofluorescence detection on one pair of clinical samples was implemented to validate the bioinformatic results. In the BC sample with high-ASCL2 expression, the intensity of red fluorescence representing CD8 protein was very weak. By contrast, the intensity of red fluorescence in the tumor sample with low-ASCL2 expression was strong (Fig. 6C). Obviously, high expression of ASCL2 was accompanied by an inhibitory infiltration of CD8 + T cells.

The immune score in high-ASCL2 expression group was significantly lower than that in low expression group, whereas the tumor purity showed an opposite trend (Fig. 6DE). Moreover, the functions of multiple immune pathways were suppressed according to the results of ssGSEA analyses, such as T cell function, cytolytic activity and antigen presentation cell (APC) function (Fig. 6F). These findings highlighted that high expression of ASCL2 may lead to an untoward status of anti-tumor immune response.

ASCL2 can suggest metabolic status and therapeutic response of breast cancer patients

Although the enrichment levels of not all metabolic gene sets were associated with ASCL2 expressions, biosynthetic process, glycolysis, amino acid (AA) metabolism, nucleotide metabolism and lipid metabolism still exhibited the trends of enrichments in the samples with high expressions (Fig. 7A-I). This indicated that high expression of ASCL2 resulted in vigorous biosynthesis, which was the biological foundation of tumor rapid growth and invasion[28].

Among commonly utilized chemotherapy and molecular targeted (MT) drugs, the sensitivity of temsirolimus, elesclomol and talazoparib was positively correlated with ASCL2 expression, while the negative correlations were observed in afatinib and lapatinib (Fig. 7JK). As for the therapeutic effects of ICIs, there was a contradiction among different bioinformatic results. TIDE scores in samples with high ASCL2 expressions were significantly higher than that in low expressions. Commonly, a higher TIDE score indicates a greater risk of immune evasion, suggesting a low chance of benefiting from immunotherapy[26]. Thus, high expression of ASCL2 indicated a poor response to immunotherapy. However, the TMB value in high expression group was markedly higher than that in

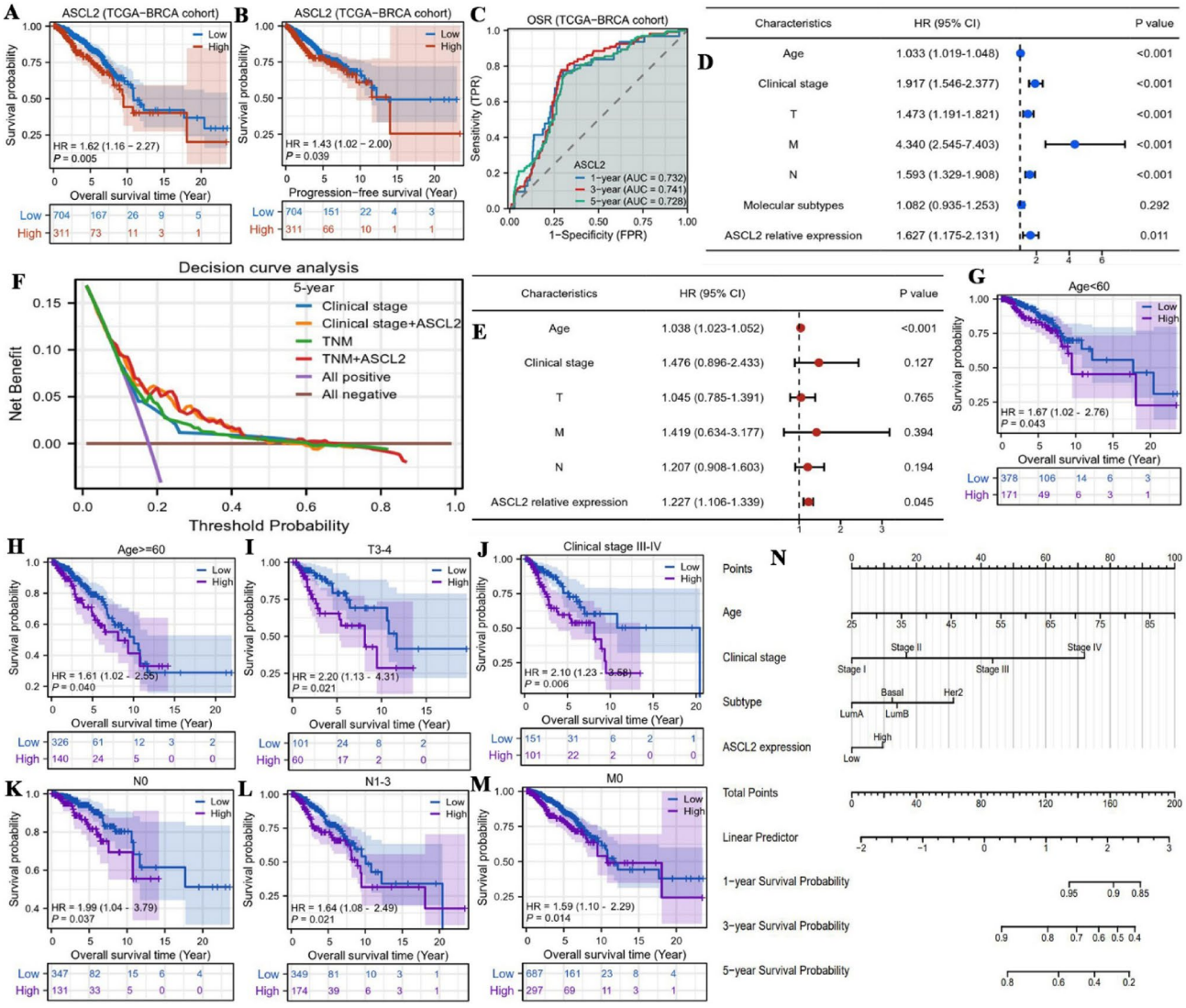

Fig. 3. Prognostic value of ASCL2 in TCGA-BRCA cohort. (**A**) Difference in OSR between high- and low-ASCL2 expression groups; (**B**) Difference in PFS between high- and low-ASCL2 expression groups; (**C**) Time-dependent accuracy of ASCL2 for predicting OSR; (**D**-**E**) The identification of BC independent prognostic factors through cox univariate (Blue) and multivariate (Red) analyses; (**F**) The decision benefit of four prognostic models based on DCA analyses; (**G**-**M**) The clinical subgroup analyses; (**N**) The nomogram consisting of clinical stage, molecular subtype and ASCL2 expression; OSR, overall survival rate; PFS, progression-free survival; HR, hazard ratio; AUC, area under curve.

low expression group and was positively correlated with ASCL2 expression (Fig. 7MN). The higher TMB value, the greater the likelihood that tumor antigens are recognized by the anti-tumor immune system, and the higher probability that immunotherapy will be effective[29]. Hence, TMB-related results indicated a favorable response to immunotherapy. Similarly, the expressions of many immune checkpoints (ICs) in high expression group were significantly higher than that in low expression group (Fig. 7O), which also supported above conclusion. Regretfully, in a real clinical cohort referring to immunotherapy (IMvigor 210 cohort), no expressive differences of ASCL2 were found between patients with different therapeutic effects (Fig. 7P).

Overexpression of ASCL2 confers higher malignancy to breast cancer

Through the PCR tests on 25 pairs of clinical samples, ASCL2 was confirmed to be significantly upregulated in tumor tissues (Fig. 8A). Prior to experiments in vitro, PCR tests determined that OE-ASCL2 and sh-ASCL2 can effectively manipulate ASCL2 expressions in MCF-7 and MDA-MB-231 cells (Fig. 8B). Colony formation assays revealed that overexpression of ASCL2 promoted, whereas silencing ASCL2 inhibited the proliferation of BC cells (Fig. 8CD). Similarly, tumor cells with ASCL2 overexpression possessed more migratory and invasive capacities, while ASCL2 deletion prevented migration and invasion processes (Fig. 8E-H).

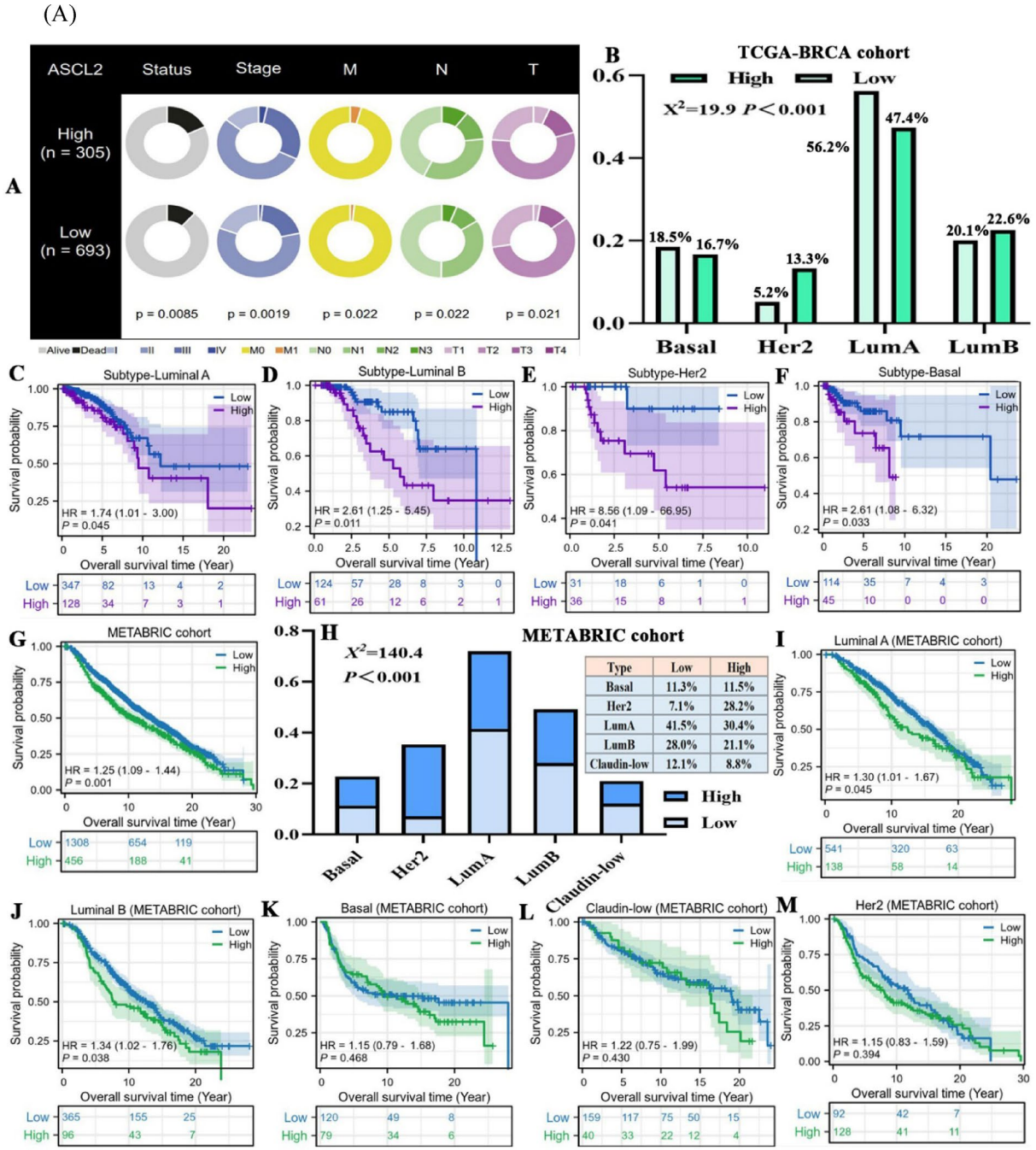

Fig. 4. Prognostic value of ASCL2 in METABRIC cohort. (**A**) The correlations between clinical features and ASCL2 expressive levels (TCGA-BRCA cohort); (**B**) Differences in the proportion of molecular subtypes between high- and low-ASCL2 expression groups (TCGA-BRCA cohort); (**C-F**) Overall survival differences of patients with four molecular subtypes between high- and low-ASCL2 expression groups (TCGA-BRCA cohort); (**G**) Overall survival differences between two ASCL2 expression groups in METABRIC cohort; (**H**) Differences in the proportion of molecular subtypes (METABRIC cohort); (I-M) Overall survival differences of patients with five molecular subtypes in METABRIC cohort.

Injection of tumor cells with ASCL2 knockdown can significantly suppress the growth of xenograft tumors in mice (Fig. 9A). The weight and volume of xenograft tumors in ASCL2 deletion group were significantly less than that in control group (Fig. 9BC). Targeting ASCL2 could be a promising therapeutic approach against BC.

The synergistic effects of ASCL2 and CLDN3 contribute to BC malignant progression

The PPI network of genes highly related to ASCL2 was constructed (Figure S2). Using the MOCDE plugin, its core module was identified, which contained CLDN3, a critical protein responsible for regulating cell tight junctions[30] (Fig. 9D). In TCGA-BRCA cohort, ASCL2 expression was highly positively correlated with CLDN3

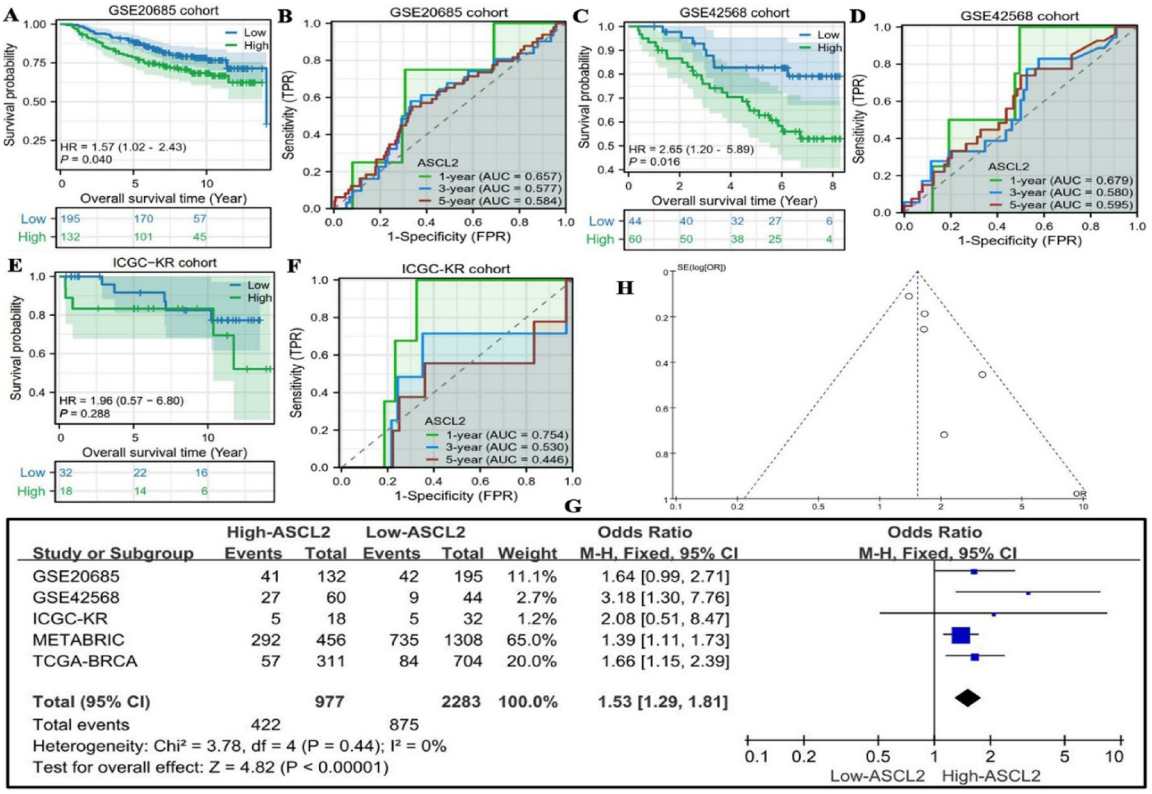

Fig. 5. Validating the prognostic value of ASCL2 in other cohorts. (**A-B**) Overall survival differences and prediction accuracy of ASCL2 in GSE20685 cohort; (**C-D**) Overall survival differences and prediction accuracy of ASCL2 in GSE42568 cohort; (**E–F**) Overall survival differences and prediction accuracy of ASCL2 in ICGC-KR cohort; (**H**) Funnel plots for assessing publication bias; (**I**) A meta-analysis for assessing the prognostic risk of high ASCL2 expression.

expression (Fig. 9E). Similar to ASCL2, high expression of CLDN3 lead to a poor survival outcome for BC patients (HR = 1.41, Fig. 9F). Hence, it was speculated that ASCL2 and CLDN3 jointly mediate the progression and metastasis of BC.

As confirmed by Western blot tests, genetic tools targeting CLDN3 can effectively alter its expressions in two BC cell lines (Fig. 10A). Co-IP assay revealed that ASCL2 was detected in the immunocomplexes pulled down by both ASCL2 and CLDN3 antibodies (Fig. 10BC). Similarly, CLDN3 can also be detected in the immunocomplexes pulled down by two antibodies (Fig. 10DE). These observations were indicative of a potential molecular interaction between ASCL2 and CLDN3. In MCF-7 cells, overexpression of CLDN3 strongly promoted cell proliferation, while ASCL2 deletion partly counteracted this facilitative effect (Fig. 10FG). In MDA-MB-231 cells, silencing CLDN3 significantly inhibited cell proliferation, while ASCL2 overexpression weakened this inhibitory effect (Fig. 10HI). As expected, overexpression of CLDN3 also enhanced the migrative and invasive abilities of MCF-7 cells, while ASCL2 knock-down impaired this reinforcement (Fig. 10JK). Targeting CLDN3 attenuated the migrative and invasive abilities of MDA-MB-231 cells, while ASCL2 overexpression rescued this weakening (Fig. 10LM). Collectively, CLDN3 possessed oncogenic functions similar to ASCL2 and cooperatively regulated the malignant behaviors of BC through molecular collaboration with ASCL2.

The pan-cancer analysis of ASCL2

We performed a preliminary pan-cancer analysis of ASCL2 to widen its biomarker availability. Among 32 cancer types in TCGA database, ASCL2 exhibited differential expressions in up to 15 cancer types, with expressive upregulations observed in all of these tumors (Fig. 11A). ASCL2 possessed prognostic value in 9 cancer types, however the impact of its high expressions on survival outcomes were closely related to the tumor types (Fig. 11B). Its high expressions were indicative of worse prognosis in four cancer types including BRCA, esophageal cancer (ESCA), lower grade glioma (LGG), and liver cancer (LIHC). Nevertheless, its high expressions revealed favorable prognosis in bladder cancer (BLCA), cervical cancer (CESC), pancreatic cancer (PAAD), stomach cancer (STAD) and melanoma (SKCM). Moreover, the close connections between ASCL2 and immune infiltration levels in almost all 31 cancer types (Fig. 11C), demonstrating its pivotal impact on the cancer tumor immune microenvironment.

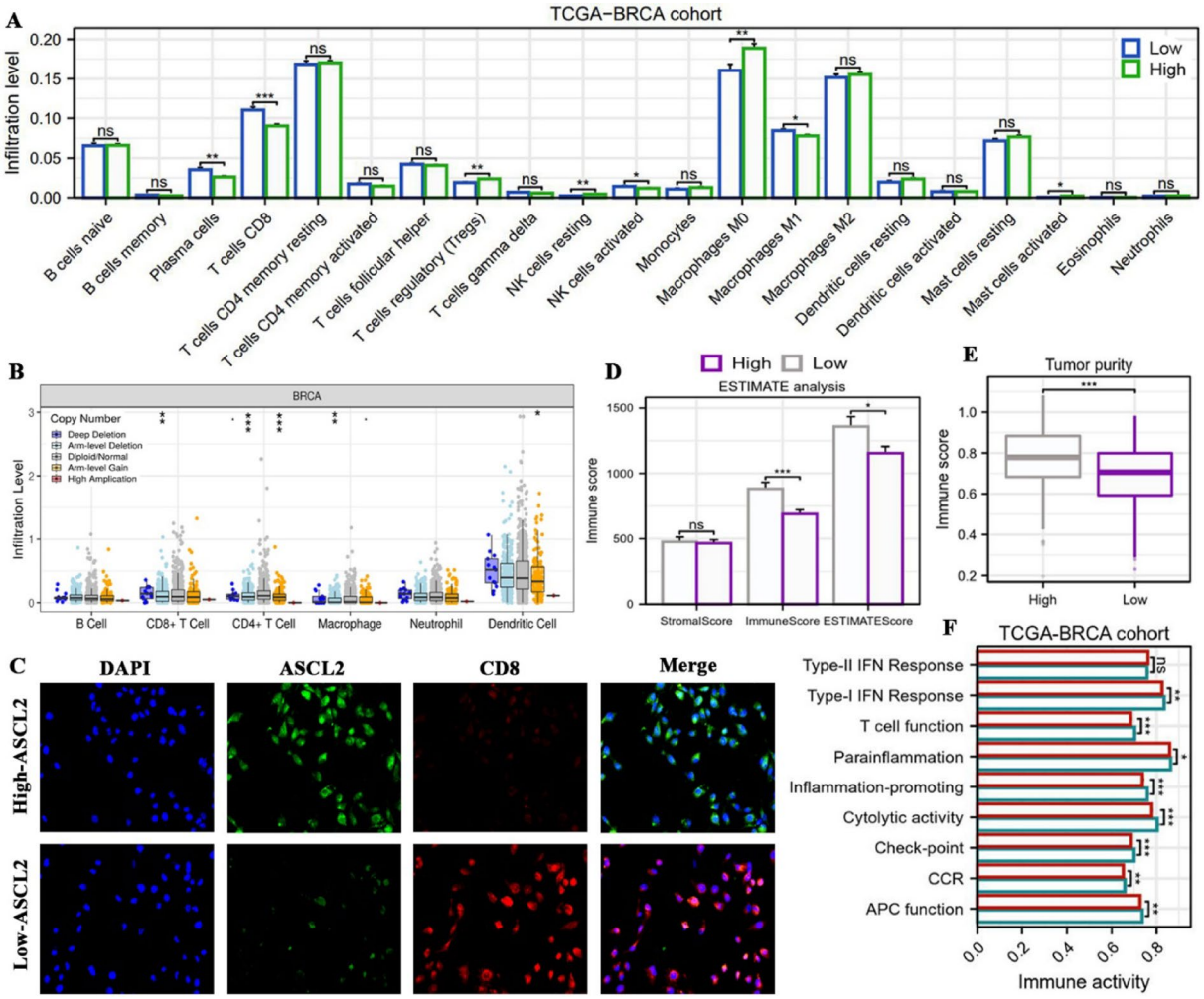

Fig. 6. The effects of ASCL2 on tumor immune microenvironment. (**A**) Differences in infiltration levels of 22 immune cells between high- and low-ASCL2 expression groups; (**B**) The associations of ASCL2 expressions with SCNAs (TIMER database); (**C**) Immunofluorescence staining on two BC samples with different ASCL2 expressions; (**D**-**E**) Differences in immune score and tumor purity between two ASCL2 expression groups based on ESTIMATE method; (**F**) Differences in activities of 10 immune signaling pathways between two ASCL2 expression groups based on ssGSEA method; SCNA, somatic copy number alteration; $^{*}P<0.05$, $^{**}P<0.01$, $^{***}P<0.001$; NS, not statistic difference.

Immune cells	Trend in high expression	Basic function	Final effect on anti-tumor immune
Plasma cells	Decreased	They primarily exert bidirectional roles in antitumor immunity through antibody secretion	Uncertain
T cells CD8	Decreased	CD8 T cells can directly kill tumor cells through the perforin-granzyme pathway and Fasl/TRAIL pathway	Unfavorable
Tregs	Increased	Tregs exert immunosuppressive effects by inhibiting the functions of T cells, NK cells, and macrophages	Unfavorable
NK cells activated	Decreased	NK cells exert rapid, non-specific cytotoxic effects in antitumor immunity, independent of antigen presentation	Unfavorable
Macrophages M0	Increased	M0 type is the common precursor of M1/M2 macrophages, and its ultimate function depends on signals from the tumor microenvironment	Uncertain
Macrophages M1	Decreased	M1-type cells can directly kill tumor cells by releasing reactive oxygen species and TNF-α, or activate T cells by presenting tumor antigens through MHC-II molecules	Beneficial
Mast cells activated	Increased	The roles of mast cells are highly dependent on the tumor microenvironment and can promote tumor progression through releasing VEGF in some cases	Unfavorable

Table 3. The effects of high ASCL2 expression on immune microenvironment. Tregs, T cells regulatory; NK, natural killer; VEGF, vascular endothelial growth factor.

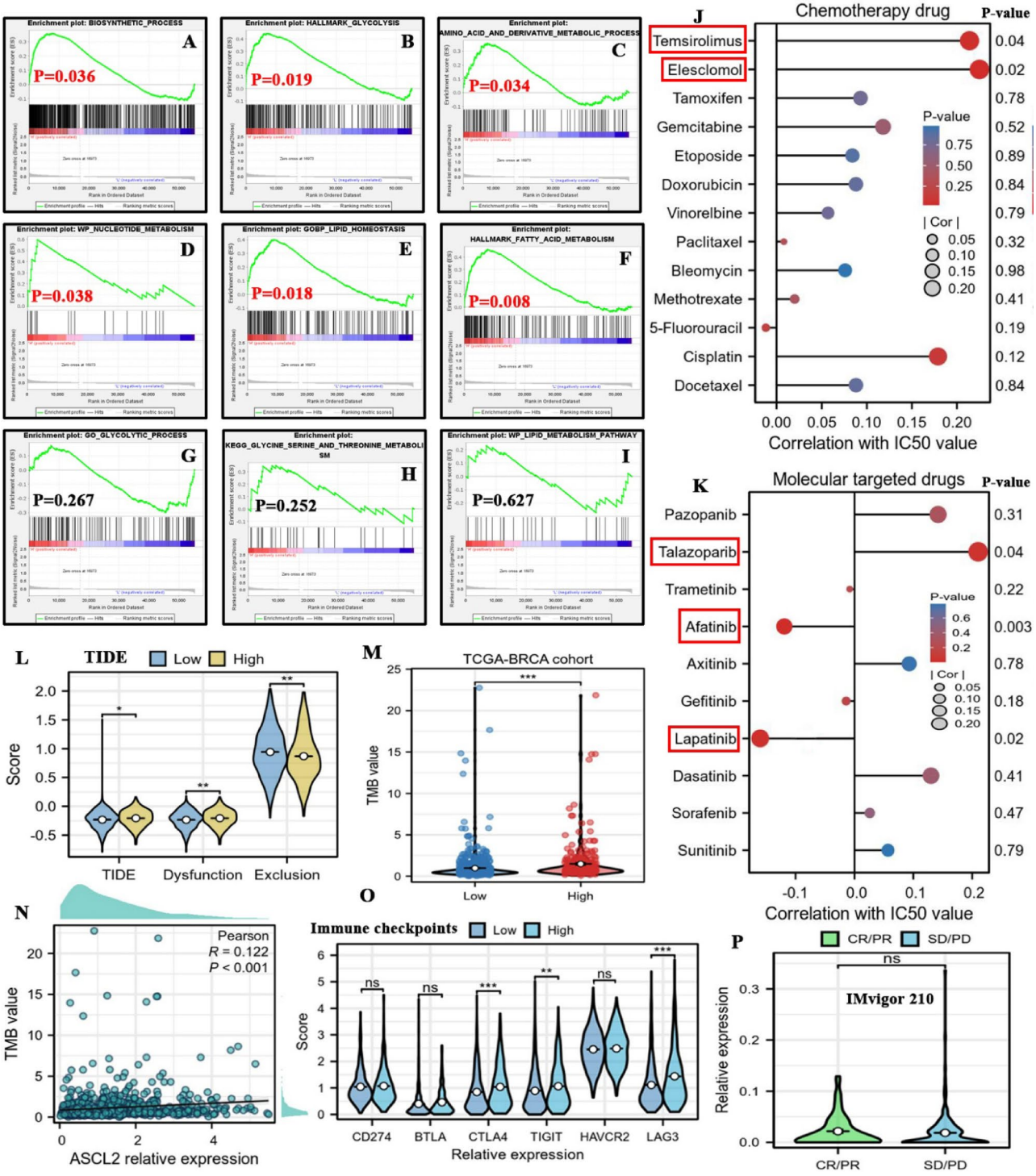

Fig. 7. The associations of ASCL2 with metabolic reprogramming and therapeutic response. (**A**-**I**) The effects of ASCL2 expressive levels on enrichments of multiple metabolic processes based on GSEA method; (**J**-**K**) The associations of ASCL2 expressions with the IC50 values of multiple common chemotherapeutics and MTT drugs (GDSC database); (**L**) Differences in TIDE scores between high- and low-ASCL2 expression groups; (**M**) Differences in TMB value; (**N**) Expressive correlation between ASCL2 and TMB value; (**O**) Expressive differences of several ICs between two ASCL2 expression groups; (**P**) The relationships between ASCL2 expressions and therapeutic responses of ICIs in IMvigor 210 cohort; IC50, half maximal inhibitory concentration; MTT, molecular targeted therapy; ICs, immune checkpoints; ICIs, immune checkpoint inhibitors; $^{*}P<0.05$, $^{**}P<0.01$, $^{***}P<0.001$; NS, not statistic difference.

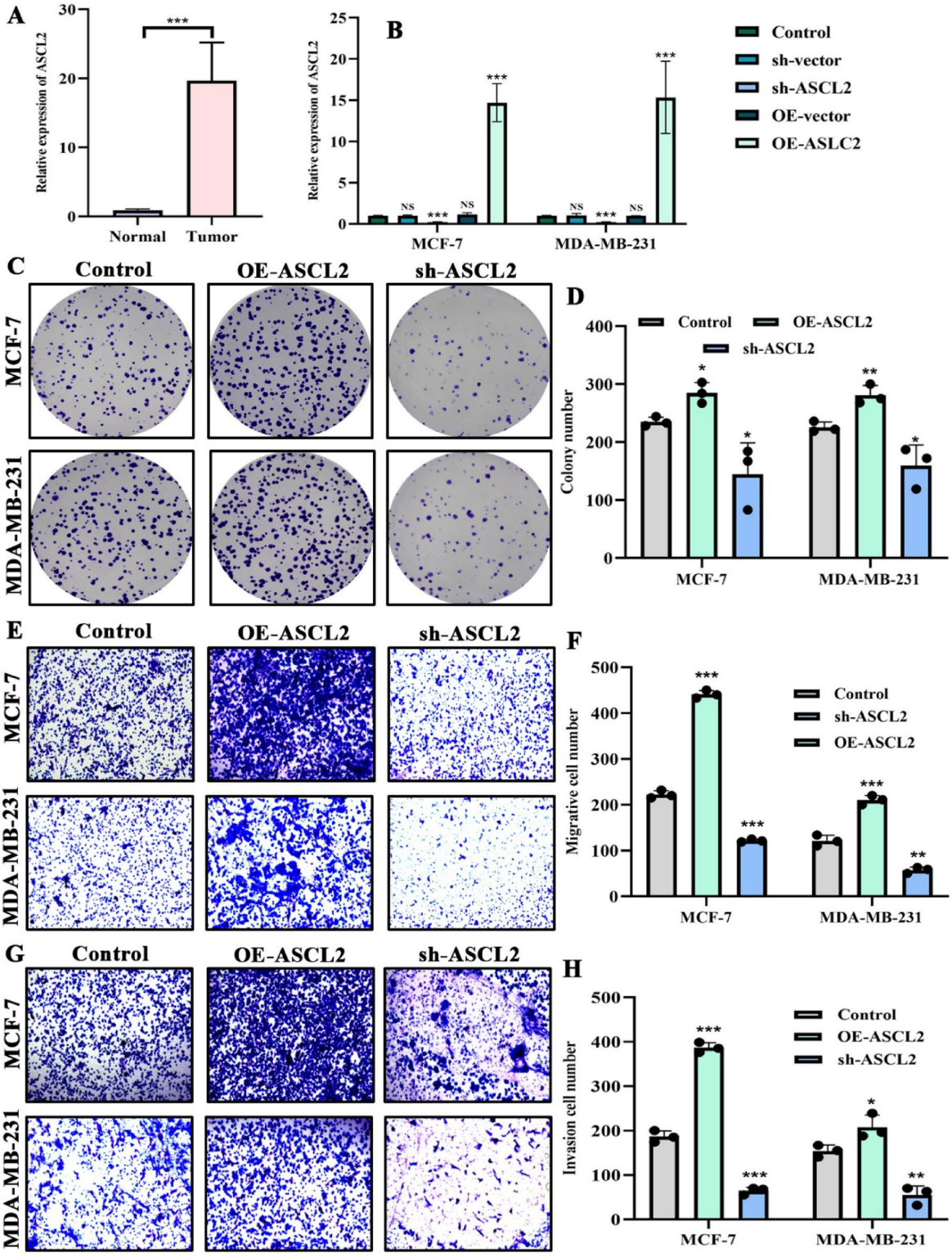

Fig. 8. The oncogenic abilities of ASCL2 in MCF-7 and MDA-MB-231 cells. (**A**) Expressive differences of ASCL2 between normal and tumor samples as determined by PCR tests; (**B**) Transfection efficiency of the recombinant vectors of ASCL2; (**C**-**D**) The effects of ASCL2 on proliferation of BC cells based on colony formation assays; (**E**–**H**) The effects of ASCL2 on migration and invasion of BC cells based on transwell assays; sh-ASCL2, the short hairpin RNA target ASCL2; OE-ASCL2, overexpression of ASCL2; $^{*}P < 0.05$, $^{**}P < 0.01$, $^{***}P < 0.001$; NS, not statistic difference.

(A)

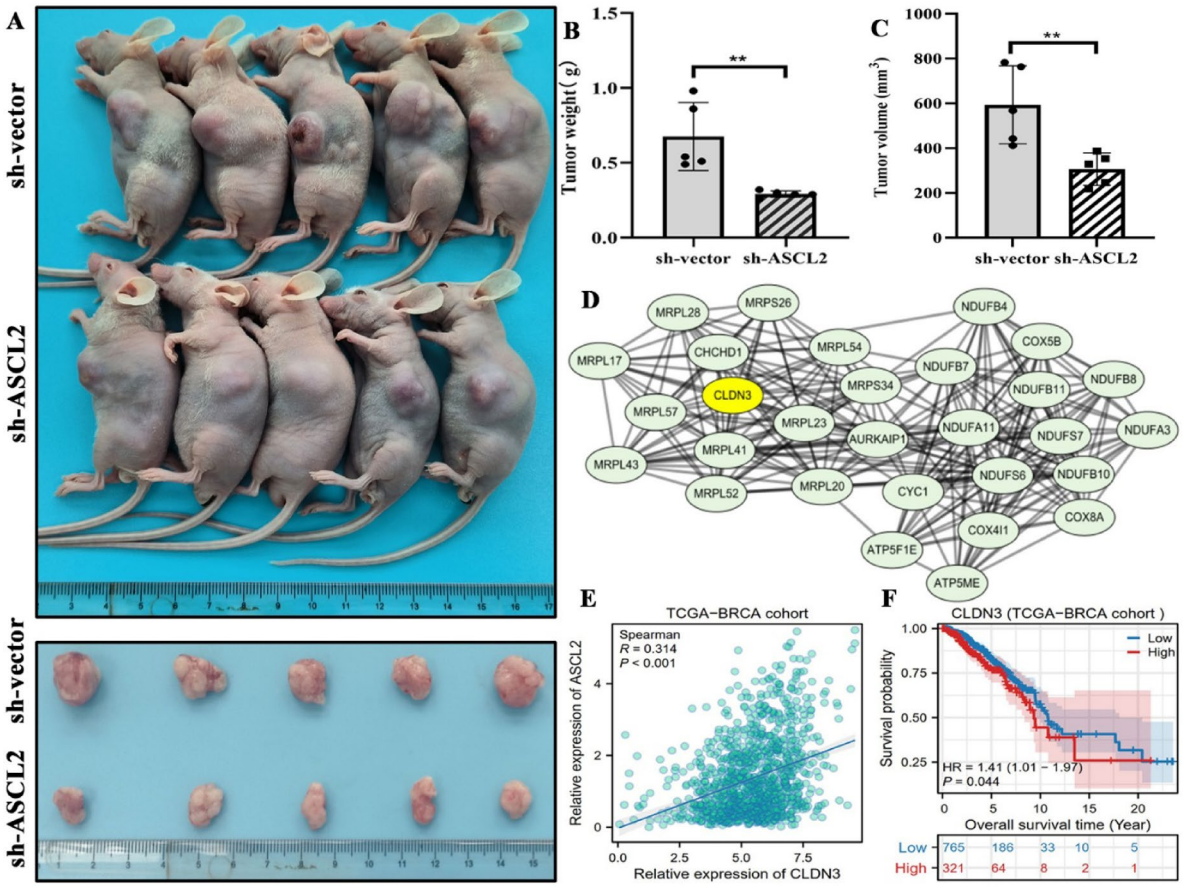

Fig. 9. The oncogenic abilities of ASCL2 in xenograft tumors in mice. (**A**) Silencing ASCL2 suppresses the growth of xenograft tumors in mice; (**B**) Differences in tumor weight between sh-vector and sh-ASCL2 groups; (**C**) Differences in tumor volumes between sh-vector and sh-ASCL2 groups; (**D**) The core module of genes that are highly related to ASCL2; (**E**) Expressive correlation between ASCL2 and CLDN3 (TCGA-BRCA cohort); (**F**) Overall survival differences between high- and low-CLDN3 expression groups (TCGA-BRCA cohort); $^{**}P < 0.01$.

The comparison between ASCL2 and other EMT biomarkers

There have been many studies identifying various EMT regulators as biomarkers for clinical assessments of BRCA[31]. Nonetheless, ASCL2 offers some advantages in some aspects (Table 4). First, excellent prediction ability. Compared with other EMT regulators, ASCL2 possessed a best prognostic analytical performance with an AUC of 0.728. Second, comprehensive bioinformatic investigation. Herein, we not only assessed the prognostic value of ASCL2, but also probed into its immune effect, metabolic influence and therapeutic correlation, comprehensively mapping its clinical landscape in BRCA. However, some studies did not even evaluate the predictive accuracy of ASCL2. Third, precise mechanism exploration. In addition to our study, the other four research did not clarify the oncogenic mechanisms of ASCL2. By contrast, we demonstrated that the synergistic effects of ASCL2 and CLDN3 exerted a pivotal role in the malignant progression of BRCA, providing valuable clues for developing therapeutic targets.

Discussion

Breast carcinoma is the most frequent malignancy diagnosed in women, leading a serious burden on public health and the economy, with 685,000 deaths annually[32]. Metastasis is its leading cause of death, up to 30% of patients are accompanied with metastatic symptoms at the time of diagnosis[33]. Although new therapeutic agents are being continuously formulated, the median OS of metastatic patients was commonly less than 60 months[34]. Therefore, elucidating the molecular mechanism of BC progression is important for its treatment. Considering EMT is the fundamental dynamic factors of tumor invasion and metastasis, we took this as a breakthrough point to attempt to provide theoretical clues for this issue. Through reasonable exploration, ASCL2 may be the answer to the question for treating BC, due to its critical clinical values and cancer regulatory capabilities.

ASCL2 is a famous transcription factor (TF) belonging to the helix-loop-helix (BHLH) family. Available evidence has demonstrated that ASCL2 can regulate cell differentiation and the origin of cancer through

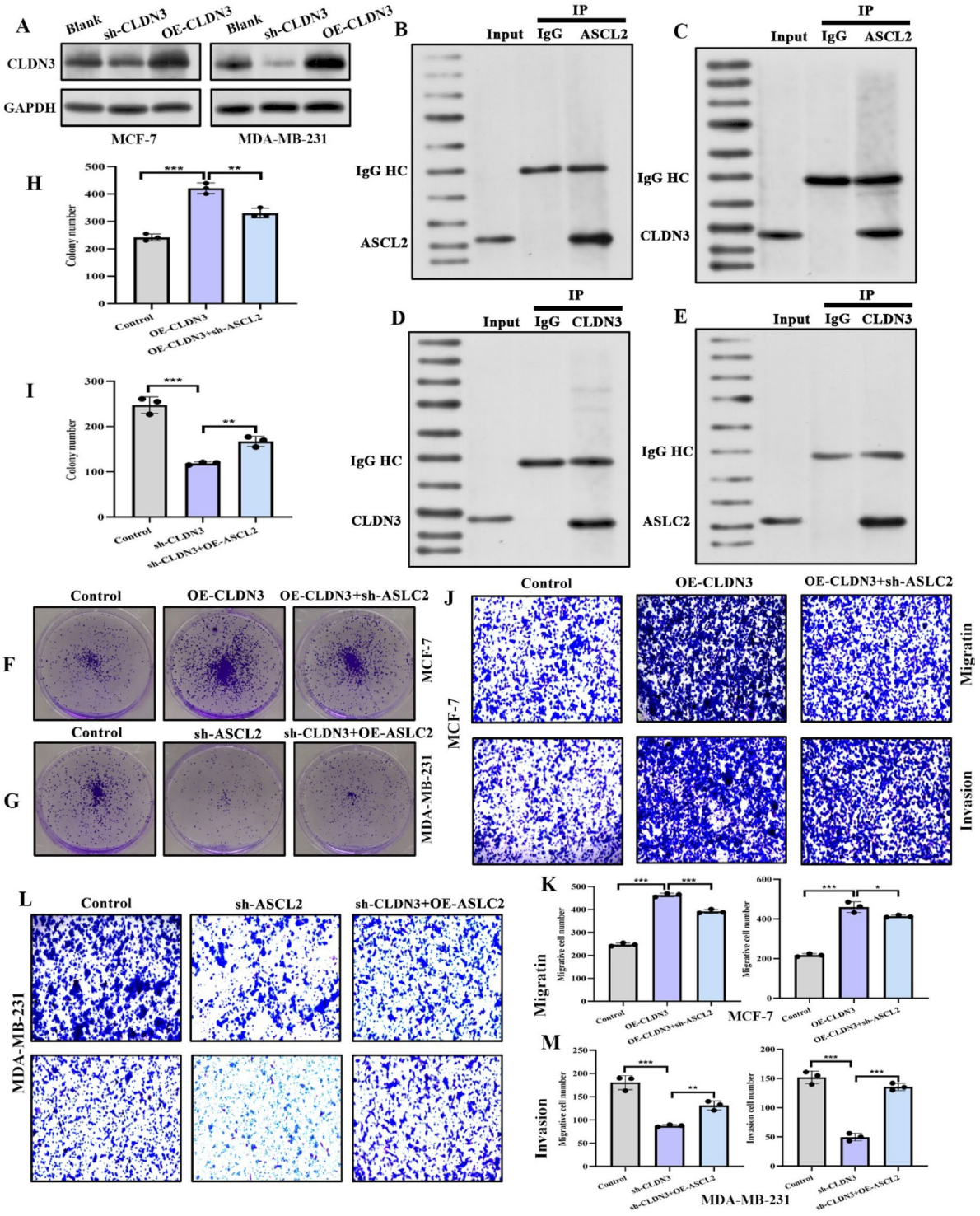

Fig. 10. An underlying oncogenic mechanism of ASCL2 in breast cancer. (**A**) Transfection efficiency of the recombinant vectors of CLDN3; (**B-E**) The interaction of ASCL2 and CLDN3 as confirmed by Co-IP assays; (**F-I**) ASCL2 and CLDN3 can mutually affect each other's ability to promote the proliferation of BC cells; (**J-M**) ASCL2 and CLDN3 can mutually affect each other's ability to promote the migration and invasion of BC cells; IP, immunoprecipitation; HC, heavy chain; LC, light chain; $^{**}P < 0.01$, $^{***}P < 0.001$.

Wnt signaling pathway[35,36]. The underlying roles of ASCL2 in tumor biology have been gradually revealed in recent years. For instance, ASCL2 contributes to gastric tumor migration, invasion and EMT process[16]. ASCL2 drives colon tumorigenesis via HMGA1-induced histone recruitment[37]. ASCL2 is a key regulator to control the neuroendocrine transition in prostate cancer[38]. These findings all pointed toward a pan-cancer property of ASCL2. Unfortunately, the research related to the roles of ASCL2 in BC is still at a relatively nascent stage. Only

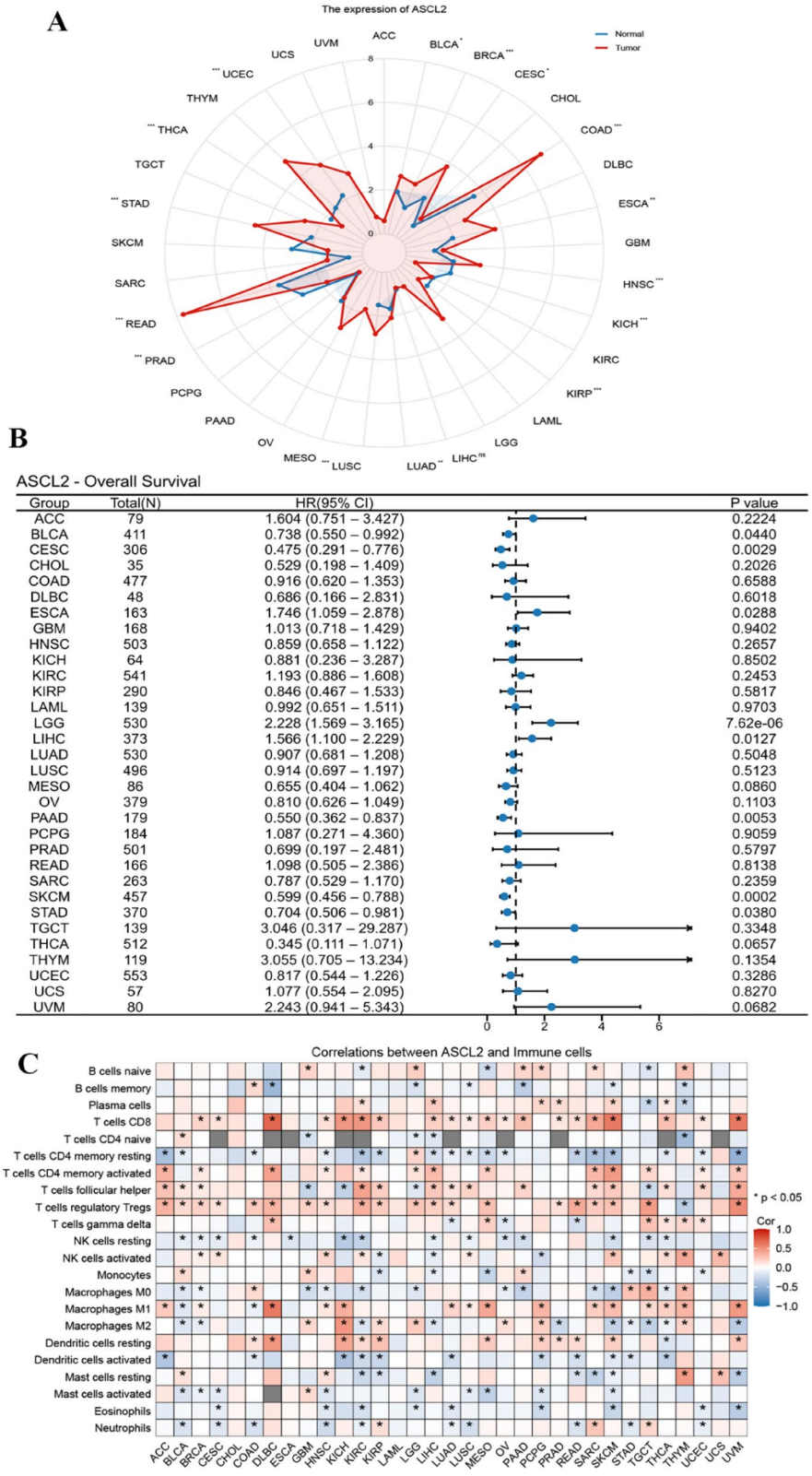

Fig. 11. Pan-cancer analysis of ASCL2. (**A**) The differential expressions of ASCL2 between normal and tumor samples across 31 cancer types in TCGA database; (**B**) The effects of ASCL2 expressive levels on the prognosis of patients across 31 cancer types; (**C**) The effects of ASCL2 expressive levels on the immune infiltration levels across 31 cancer types. $^{*}P<0.05$, $^{**}P<0.01$, $^{***}P<0.001$; NS, not statistic difference.

Study PMID	Gene	Validation cohort	Prediction accuracy	Mechanism exploration
40,634,441	NOX4	NA	NA	NA
37,304,008	EZR	Three ($n=2091$)	0.693	NA
36,620,876	CBX3	NA	0.664	NA
30,602,372	PRAME	NA	NA	NA
NA	ASCL2	Four ($n=2245$)	0.728	Synergistic function of CLDN3

Table 4. The comparison between ASCL2 and other EMT biomarkers. NA, not applicable.

one study observed that elevated ASCL2 expression was closely associated with worse prognosis in BC[39]. Herein, we demonstrated that ASCL2 promoted malignant capacities of BC cells, and silencing ASCL2 can significantly inhibit the growth of xenograft tumors in mice. It refines the functional landscape of ASCL2 in human cancers. Targeting ASCL2 has the potential to be a promising approach for fighting BC. Indeed, AT7867, a potent oral AKT inhibitor has been experimentally confirmed to suppress stemness and progression of colorectal cancer (CRC) through targeting ASCL2[40].

ASCL2-involved carcinogenesis implicates intricate regulatory mechanisms. In the post-transcriptional regulation, TET2-BCLAF1 complex can up-regulate the methylation of ASCL2 promoter, thereby inhibiting ASCL2 expression and colorectal cancer progression[41]. In the transcriptional regulation, SMYD3 can be transcriptionally activated by the TCF4 complex, thereby promoting ASCL2 expression via enhancing its H3K4me3 status[42]. Here, we identified a novel access to regulate BC progression, termed the synergistic effect of ASCL2 and CLDN3. Co-IP assays confirmed the existence of direct or indirect interaction between them, while the rescue experiments demonstrated that they can mutually affect each other's oncogenic abilities. In fact, multiple oncogenes mediate cancer progression by establishing interactions with other molecules. For instance, FNDC3B can facilitate gastric cancer metastasis via interacting with FAM83H[43]. DAB2 binding to LASP1 strongly promotes the migration and invasion of non-small cell lung cancer (NSCLC)[44]. Clearly, our findings will open up new perspectives on BC treatments.

Accurate clinical assessment is a critical issue in cancer individualized therapy. As the most widely used prognostic tool, the C-index of TNM staging system is just 0.716, which has plenty of room for improvement[45]. Through our comprehensive investigation, ASCL2 not only possessed an excellent prediction accuracy, but also lifted the decision performance of TNM system. Thus, ASCL2 is an important complement to the TNM-based prognostic evaluation system. An increasing number of scholars have advocated incorporating biological factors into the prognostic system, which leads the future trend[46]. Moreover, ASCL2 promises to be a reliable biomarker for reflecting the metabolic, immune and therapeutic status of BC, which was partly supported by the existing research. For instance, ASCL2 can induce immune tolerant microenvironment through recruiting cancer-associated fibroblasts[9]. ASCL2-DPEP1 positive feedback loop facilitates drug resistance in colon cancer[47]. Altogether, ASCL2 has great potential to display the clinical status of BC using genetic information.

Our bioinformatic findings revealed that the prognostic performance of ASCL2 in validation cohorts was slightly weaker than that in TCGA cohort. There are two possible reasons for this limitation. First, the biological heterogeneity. There are certain differences in clinical characteristics among patients in different cohorts, which leads to a substantial variation in the biological effects of ASCL2 across different tumor samples, thereby resulting in prognostic differences[48]. For example, up to 23.8% (265/1109) of patients were diagnosed with middle or advanced stage disease in TCGA cohort, whereas this proportion was only 12% (6/50) in ICGC cohort. Moreover, the mean age of patients in ICGC cohort was obviously younger than that in the other cohorts (31.81 vs 58.83), which may indicate a higher malignant cancer potential. Second, the heterogeneity of techniques and methodologies. For example, the discrepancies in tumor tissue collection, fixation, and preservation across different cohorts can significantly affect RNA quality, thereby affecting the measurements of ASCL2 expressions[49]. Additionally, different sequencing platforms vary in their sensitivity, dynamic range, and background noise for detecting gene expression levels. These technical factors will all influence the ultimate assessments of ASCL2's prognostic performance. To better move ASCL2 as an effective prognostic marker in clinical practice, two points are worth noting. First, from a single marker to a combined model. Although ASCL2 exhibited a certain prognostic analytic capability, it is not realistic to expect that ASCL2 individually undertakes the precise prognostic assessment of BRCA. Constructing a comprehensive model by combining it with classic indicators such as TNM staging is a more appropriate approach[50]. Second, validation in large, prospective, heterogeneous cohorts. The small and retrospective cohorts should be banished in favor of robust large-scale data to refine the prognostic parameters of ASCL2, such as the determination of cutoff value and applicable subgroup populations.

ASCL2 and CLDN3 synergistically drive malignant progression of BRCA through specific molecular pathways. On one hand, as a TF, ASCL2 can active multiple effector molecules of Wnt/β-catenin signaling pathway, such as TWIST[16] and ZEB1[51], thereby promoting EMT process. On the other hand, CLDN3 serves as a core protein component of cell tight junctions[30]. Its aberrant expressions in cancers will lead to loss of cell polarity and the defects in intercellular adhesion function, thereby enhancing the invasive capacity of tumor cells[52]. This alteration of adhesion property is complementary to the mesenchymal phenotype driven by ASCL2, together facilitating tumor metastasis.

Naturally, there are still several limitations to this study. First, the prognostic value of ASCL2 has not been adequately tested in more clinical cohorts. The nomogram constructed by ASCL2 also lacked clinical validation in predicting OSR of patients. Second, the associations of ASCL2 with cancer metabolism and therapeutic

response were not verified by cell experimentations and clinical data. Third, evidence has been presented that ASCL2 is a pivotal downstream target gene of Wnt signaling pathway. Nevertheless, it remains elusive whether the synergistic molecular of ASCL2, CLDN3, is also activated by the Wnt pathway. Thus, further research is necessary to address the above inadequacies.

Conclusion

Distant metastasis is the leading cause of death in BC patients, the overall survival for advanced patients is commonly less than 5 years. EMT is an essential process for cancer development and progression, providing a promising solution to BC treatment. Herein, a critical regulator ASCL2 was confirmed to have a high value in BC clinical assessments, due to its suggestive roles in prognosis, anti-tumor immune response, metabolism reprogramming and therapeutic efficacy. Through a series of in vitro and in vivo experimentations, ASCL2 exhibited potent oncogenic effects and targeting it is expected to be a promising strategy. Mechanistically, the synergistic effects of ASCL2 and CLDN3 mediated malignant progression of BC. Collectively, our findings will provide new insights into BC personalized therapy.

Availability of data and materials

The datasets used and/or analyzed in the current study are available from the corresponding author upon reasonable request.

Received: 26 June 2025; Accepted: 17 November 2025
Published online: 29 November 2025

References

1. Giaquinto, A. N. et al. Breast cancer statistics 2024. *CA: a Cancer J. Clin.* **74**(6), 477–95 (2024).
2. Xu, F., Fu, H. & Ma, J. Multifaceted efforts of governments, medical institutions, and financial organizations contribute to reducing the health inequality caused by economic differences. *Cancer Biol. Med.* **21**, 1100–1103 (2024).
3. Cortes, J. et al. Pembrolizumab plus chemotherapy versus placebo plus chemotherapy for previously untreated locally recurrent inoperable or metastatic triple-negative breast cancer (KEYNOTE-355): a randomised, placebo-controlled, double-blind, phase 3 clinical trial. *Lancet (London, England).* **396**(10265), 1817–1828 (2020).
4. Tomecka, P. et al. Factors Determining Epithelial-Mesenchymal Transition in Cancer Progression. *Int. J. Mol. Sci.* **25**(16), 8972 (2024).
5. Hariri, A. et al. Intersecting pathways: The role of hybrid E/M cells and circulating tumor cells in cancer metastasis and drug resistance Drug resistance updates : reviews and commentaries in antimicrobial and anticancer chemotherapy. *Drug Res. Updat.* **76**, 101119 (2024).
6. Li, W. et al. PD-L1 knockdown suppresses vasculogenic mimicry of non-small cell lung cancer by modulating ZEB1-triggered EMT. *BMC Cancer* **24**(1), 633 (2024).
7. Li, F., Wang, J., Yan, Y. Q., Bai, C. Z. & Guo, J. Q. CD147 promotes breast cancer migration and invasion by inducing epithelial-mesenchymal transition via the MAPK/ERK signaling pathway. *BMC Cancer* **23**(1), 1214 (2023).
8. Wang, X. et al. Epithelial-mesenchymal plasticity in cancer: signaling pathways and therapeutic targets. *MedComm.* **5**(8), e659 (2024).
9. Zhang, D. et al. ASCL2 induces an immune excluded microenvironment by activating cancer-associated fibroblasts in microsatellite stable colorectal cancer. *Oncogene* **42**(38), 2841–2853 (2023).
10. Wu, L. et al. ASCL2 Affects the Efficacy of Immunotherapy in Colon Adenocarcinoma Based on Single-Cell RNA Sequencing Analysis. *Front. Immunol.* **13**, 829640 (2022).
11. Wu, C. Y., Tsai, Y. P., Wu, M. Z., Teng, S. C. & Wu, K. J. Epigenetic reprogramming and post-transcriptional regulation during the epithelial-mesenchymal transition. *Trends in genetics : TIG.* **28**(9), 454–463 (2012).
12. Beyes, S. et al. Genome-wide mapping of DNA-binding sites identifies stemness-related genes as directly repressed targets of SNAIL1 in colorectal cancer cells. *Oncogene* **38**(40), 6647–6661 (2019).
13. Veerasamy, M., Phanish, M. & Dockrell, M. E. Smad mediated regulation of inhibitor of DNA binding 2 and its role in phenotypic maintenance of human renal proximal tubule epithelial cells. *PLoS ONE* **8**(1), e51842 (2013).
14. Cubillo, E. et al. E47 and Id1 interplay in epithelial-mesenchymal transition. *PLoS ONE* **8**(3), e59948 (2013).
15. Sun, B., Zhang, D., Zhao, N. & Zhao, X. Epithelial-to-endothelial transition and cancer stem cells: two cornerstones of vasculogenic mimicry in malignant tumors. *Oncotarget* **8**(18), 30502–30510 (2017).
16. Zuo, Q. et al. ASCL2 expression contributes to gastric tumor migration and invasion by downregulating miR223 and inducing EMT. *Mol. Med. Rep.* **18**(4), 3751–3759 (2018).
17. Shang, Y. et al. HIF-1α/Ascl2/miR-200b regulatory feedback circuit modulated the epithelial-mesenchymal transition (EMT) in colorectal cancer cells. *Exp. Cell Res.* **360**(2), 243–256 (2017).
18. Vasaikar, S. V. et al. EMTome: a resource for pan-cancer analysis of epithelial-mesenchymal transition genes and signatures. *Br. J. Cancer* **124**(1), 259–269 (2021).
19. Zhou, Y. et al. Metascape provides a biologist-oriented resource for the analysis of systems-level datasets. *Nat. Commun.* **10**(1), 1523 (2019).
20. Xu, F., Zhang, P., Yuan, M., Yang, X. & Chong, T. Bioinformatic screening and identification of downregulated hub genes in adrenocortical carcinoma. *Exp. Ther. Med.* **20**(3), 2730–2742 (2020).
21. Yoshihara, K. et al. Inferring tumour purity and stromal and immune cell admixture from expression data. *Nat. Commun.* **4**, 2612 (2013).
22. Xu, F. et al. SLC1A5 Prefers to Play as an Accomplice Rather Than an Opponent in Pancreatic Adenocarcinoma. *Front. Cell Dev. Biol.* **10**, 800925 (2022).
23. Xu, F. et al. The impact of TNFSF14 on prognosis and immune microenvironment in clear cell renal cell carcinoma. *Genes & Genom.* **42**(9), 1055–1066 (2020).
24. Xu, F. et al. N7-methylguanosine regulatory genes well represented by METTL1 define vastly different prognostic, immune and therapy landscapes in adrenocortical carcinoma. *Am. J. Cancer Res.* **13**(2), 538–568 (2023).
25. Xu, F. et al. Tumor mutational burden presents limiting effects on predicting the efficacy of immune checkpoint inhibitors and prognostic assessment in adrenocortical carcinoma. *BMC Endocr. Disord.* **22**(1), 130 (2022).
26. Jiang, P. et al. Signatures of T cell dysfunction and exclusion predict cancer immunotherapy response. *Nat. Med.* **24**(10), 1550–1558 (2018).
27. Snyder, A. et al. Contribution of systemic and somatic factors to clinical response and resistance to PD-L1 blockade in urothelial cancer: An exploratory multi-omic analysis. *PLoS Med.* **14**(5), e1002309 (2017).

28. Fu, W., Sun, A. & Dai, H. Lipid metabolism involved in progression and drug resistance of breast cancer. *Genes & Dis.* **12**(4), 101376 (2025).
29. Dvir, K., Giordano, S. & Leone, J. P. Immunotherapy in Breast Cancer. *Int. J. Mol. Sci.* **25**(14), 7517 (2024).
30. Wang, W., Zhou, Y., Li, W., Quan, C. & Li, Y. Claudins and hepatocellular carcinoma. *Biomed. & Pharmacother. = Biomed. & Pharmacother.* **171**, 116109 (2024).
31. Sun, J. et al. NOX4 serves as a pan-cancer prognostic biomarker and therapeutic target in tumorigenesis. *Sci. Rep.* **15**(1), 24612 (2025).
32. Wang, W. et al. Global, regional, and national burden of breast cancer in young women from 1990 to 2021: findings from the global burden of disease study 2021. *BMC Cancer* **25**(1), 1015 (2025).
33. Wasilewski, D. et al. Re-resection of brain metastases - outcomes of an institutional cohort study and literature review. *BMC Cancer* **25**(1), 973 (2025).
34. Kesireddy, M. et al. Overall Survival and Prognostic Factors in De Novo Metastatic Human Epidermal Growth Factor Receptor (HER)-2-Positive Breast Cancer: A National Cancer Database Analysis. *Cancers* **17**(11), 1823 (2025).
35. Murata, K. et al. Ascl2-Dependent Cell Dedifferentiation Drives Regeneration of Ablated Intestinal Stem Cells. *Cell Stem Cell* **26**(3), 377–90.e6 (2020).
36. Nagae, G. et al. Genetic and epigenetic basis of hepatoblastoma diversity. *Nat. Commun.* **12**(1), 5423 (2021).
37. Luo, L. Z., Kim, J. H., Herrera, I., Wu, S., Wu, X., Park. S. S., et al. HMGA1 acts as an epigenetic gatekeeper of ASCL2 and Wnt signaling during colon tumorigenesis. J. Clin. Investigation. **135**(3) (2025)
38. Chen, C. C. et al. Temporal evolution reveals bifurcated lineages in aggressive neuroendocrine small cell prostate cancer transdifferentiation. *Cancer Cell* **41**(12), 2066–82.e9 (2023).
39. Xu, H. et al. Elevated ASCL2 expression in breast cancer is associated with the poor prognosis of patients. *Am. J. Cancer Res.* **7**(4), 955–961 (2017).
40. Li, Y. et al. AT7867 Inhibits the Growth of Colorectal Cancer Stem-Like Cells and Stemness by Regulating the Stem Cell Maintenance Factor Ascl2 and Akt Signaling. *Stem Cells Int.* **2023**, 4199052 (2023).
41. Shang, Y. et al. TET2-BCLAF1 transcription repression complex epigenetically regulates the expression of colorectal cancer gene Ascl2 via methylation of its promoter. *J. Biol. Chem.* **298**(7), 102095 (2022).
42. Wang, T. et al. SMYD3 controls a Wnt-responsive epigenetic switch for ASCL2 activation and cancer stem cell maintenance. *Cancer Lett.* **430**, 11–24 (2018).
43. Zhang, Y. et al. FNDC3B promotes gastric cancer metastasis via interacting with FAM83H and preventing its proteasomal degradation. *Cell. Mol. Biol. Lett.* **30**(1), 65 (2025).
44. Li, Q., Zeng, S., Long, H., He, Y., Tu, R., Li, Y. et al. DAB2 binds to LASP1 to participate in migration and invasion of non-small cell lung cancer through TGF-β/Smad pathway. J. Formosan Med. Assoc. = Taiwan yi zhi. (2025).
45. Li, X. et al. Validation of the newly proposed American Joint Committee on Cancer (AJCC) breast cancer prognostic staging group and proposing a new staging system using the National Cancer Database. *Breast Cancer Res. Treat.* **171**(2), 303–313 (2018).
46. Weiss, A., King, T. A., Hunt, K. K. & Mittendorf, E. A. Incorporating Biologic Factors into the American Joint Committee on Cancer Breast Cancer Staging System: Review of the Supporting Evidence. *Surg. Clin. North Am.* **98**(4), 687–702 (2018).
47. Zeng, C. et al. DPEP1 promotes drug resistance in colon cancer cells by forming a positive feedback loop with ASCL2. *Cancer Med.* **12**(1), 412–424 (2023).
48. Ho, J. et al. Translational genomics in pancreatic ductal adenocarcinoma: A review with re-analysis of TCGA dataset. *Semin. Cancer Biol.* **55**, 70–77 (2019).
49. Li, L. et al. What are the applications of single-cell RNA sequencing in cancer research: a systematic review. *J. Exp. & Clin. Cancer Res. : CR.* **40**(1), 163 (2021).
50. Xu, F., Li, Z., Guan, H. & Ma, J. Multiple machine learning algorithms, validation of external clinical cohort and assessments of model gain effects will better serve cancer research on bioinformatic models. *Cancer Cell Int.* **24**(1), 427 (2024).
51. Rönsch, K. et al. SNAIL1 combines competitive displacement of ASCL2 and epigenetic mechanisms to rapidly silence the EPHB3 tumor suppressor in colorectal cancer. *Mol. Oncol.* **9**(2), 335–354 (2015).
52. Cox, K. E. et al. The Expression of the Claudin Family of Proteins in Colorectal Cancer. *Biomolecules.* **14**(3), 272 (2024).

Acknowledgements
All authors would like to thank the Second Affiliated Hospital of Xi'an Jiaotong University and Dr. Fangshi Xu for their support.

Author contributions
YGL conceived and designed the study. YLY, QJM, XHL and FSX analyzed and interpreted the data. YLY, QJM, XHL, FSX, YWL, XGH and QQG wrote the manuscript. YLY, QJM, XHL, FSX and YWL conducted in vitro and in vivo experiments. YGL, YLY and QJM made revised version. All authors have read and approved the manuscript.

Funding
The authors declare that no financial support was received for the research and/or publication of this article.

Declarations

Competing interests
The authors declare that they have no competing interests.

Ethics approval and informed consent
This study was reviewed and approved by the Ethics Committee of Xi'an No.3 Hospital (ID:20,230,416). We confirmed that all methods were performed in accordance with the relevant guidelines and regulations. We confirm that all methods are reported in accordance with ARRIVE guidelines.

Consent for publication
For ASCL2 testing on clinical samples, the patients provided written informed consent.

Additional information

Supplementary Information The online version contains supplementary material available at https://doi.org/10.1038/s41598-025-29350-2.

Correspondence and requests for materials should be addressed to Y.L.

Reprints and permissions information is available at www.nature.com/reprints.

Publisher's note Springer Nature remains neutral with regard to jurisdictional claims in published maps and institutional affiliations.